A Spectral Element DG Method for the Vlasov–Poisson Equation

Éric Madaule[a], Marco Restelli[a], Eric Sonnendrücker[a]

[a] Numerische Methoden in der Plasmaphysik, Max–Planck–Institut für Plasmaphysik, Garching bei München, Germany.

Overview

- Spectral Element (SE) Discontinuous Galerkin (DG) method for the Vlasov–Poisson (VP) equation
- Energy conserving approximation of the electric field
- Time integration schemes: Runge–Kutta (RK) methods vs. exponential integrators
- Numerical validation
  - linear and nonlinear Landau damping
  - “bump on tail” test case
  - two-stream instability

Introduction (I)

We consider the VP equation

$$\begin{cases} \partial_t f + \underline{v} \cdot \nabla_x f - \underline{E} \cdot \nabla_v f &= 0 \\ \nabla \cdot \underline{E} &= 1 - \rho, \end{cases}$$

closely following *[Ayuso, Carrillo, Shu, 2011]*, *[Ayuso, Hajian, 2012]* and *[Ayuso, Carrillo, Shu, 2012]* and introducing the following original elements:

- spectral element formulation
- energy conservation using a local reconstructions of $\underline{E}$, obtained solving a unique Poisson problem
- preliminary experiments considering exponential time integrators.

Introduction (II)

More precisely, we consider

$$\partial_t f + \underline{v} \cdot \nabla_x f - \underline{E} \cdot \nabla_v f = 0 \quad \text{in} \quad \Omega \times [0\,, T], \tag{1}$$

$$\begin{aligned} \nabla \cdot \underline{E} &= 1 - \rho \\ \underline{E} - \nabla \Phi &= 0 \end{aligned} \quad \text{in} \quad \Omega_x \times [0\,, T], \tag{2}$$

$$\rho(t, \underline{x}) = \int_{\Omega_v} f(t, \underline{x}, \underline{v})\, \mathrm{d}\underline{v}, \tag{3}$$

with $\Omega = \Omega_x \times \Omega_v$ and $\Omega_x, \Omega_v \subset \mathbb{R}^d$, for $d \geq 1$.

We assume that both Ω_x and Ω_v are rectangles in $\mathbb{R}^d$ and consider periodic boundary conditions for simplicity.

Introduction (III)

The continuous problem is characterized by:

- particle conservation

$$\iint_{\Omega} f \, \mathrm{d}\underline{x} \, \mathrm{d}\underline{v} = const \tag{4}$$

- momentum conservation

$$\iint_{\Omega} \underline{v} f \, \mathrm{d}\underline{x} \, \mathrm{d}\underline{v} = const \tag{5}$$

- energy conservation

$$\int_{\Omega_x} \left[\int_{\Omega_v} f \frac{v^2}{2} \mathrm{d}\underline{v} + \frac{E^2}{2} \right] \mathrm{d}\underline{x} = const \tag{6}$$

- positivity of the solution

$$f(t, \underline{x}, \underline{v}) \geq 0. \tag{7}$$

Introduction (IV)

The considered SE-DG scheme provides:

- high-order accuracy $\mapsto$ spectral element
- numerical stability $\mapsto$ upwind
- particle conservation $\mapsto$ DG
- energy conservation $\mapsto$ suitable reconstruction for $\underline{E}$
- efficiency and scalability $\mapsto$ SE-DG, Cartesian
- flexibility $\mapsto$ nonuniform grid ($+$ noncoforming grids).

It is still an open problem how to deal with:

- momentum conservation
- positivity of the numerical solution.

DG formulation (I)

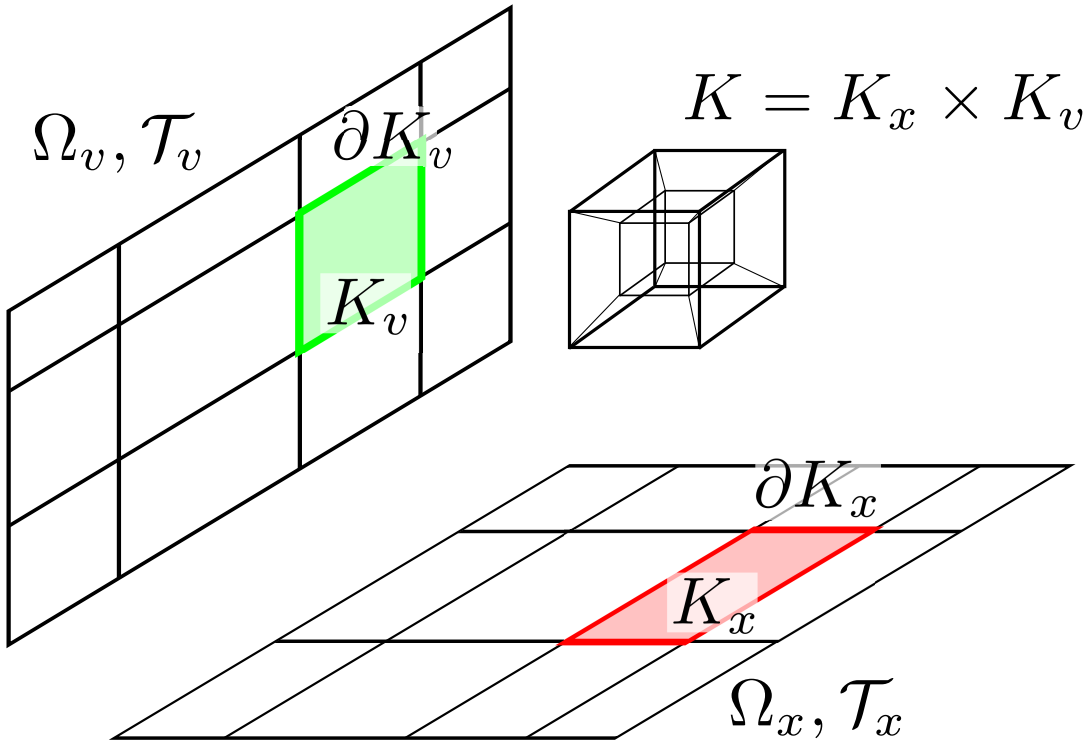

$$\partial_x K = \partial K_x \times K_v$$
$$\partial_v K = K_x \times \partial K_v$$

$$\{\phi\} = \frac{1}{2}(\phi + \phi'), \qquad [\![\phi]\!] = \phi \underline{n} + \phi' \underline{n}',$$

$$\{\underline{q}\} = \frac{1}{2}(\underline{q} + \underline{q}'), \qquad [\![\underline{q}]\!] = \underline{q} \cdot \underline{n} + \underline{q}' \cdot \underline{n}'.$$

DG formulation (II)

For each element $K \in \mathcal{T}$:

- define a local polynomial space $V(K) = \mathbb{P}_k(K)$
- multiply the VP equation by $u \in V(K)$, integrate over K
- integrate by parts and substitute the boundary terms with the corresponding numerical fluxes, yielding

$$\iint_K f_t u \,\mathrm{d}\underline{x}\,\mathrm{d}\underline{v} - \iint_K \underline{v} f \cdot \nabla_x u \,\mathrm{d}\underline{x}\,\mathrm{d}\underline{v} + \int_{\partial_x K} \underline{n} \cdot \widehat{\underline{v} f} u \,\mathrm{d}\sigma\,\mathrm{d}\underline{v}$$

$$+ \iint_K \underline{\tilde{E}} f \cdot \nabla_v u \,\mathrm{d}\underline{x}\,\mathrm{d}\underline{v} - \int_{\partial_v K} \underline{n} \cdot \widehat{\underline{E} f} u \,\mathrm{d}\underline{x}\,\mathrm{d}\tau = 0,$$

where $\widehat{\cdot}$ denotes the numerical fluxes, $f|_K \in V(K)$ and $\underline{\tilde{E}}$ is an approximation of the electric field to be defined later.

DG as high-order FV

The DG method can be regarded as a high-order extension of the finite volume method.
As such, it provides naturally the following properties:

- particle conservation: taking $u = 1_K$ yields

$$\iint_K f_t \,\mathrm{d}\underline{x}\,\mathrm{d}\underline{v} = -\int_{\partial_x K} \underline{n}\cdot\widehat{\underline{v}f}\,\mathrm{d}\sigma\,\mathrm{d}\underline{v} + \int_{\partial_v K} \underline{n}\cdot\widehat{\underline{E}f}\,\mathrm{d}\underline{x}\,\mathrm{d}\tau$$

- numerical diffusion proportional to $[\![f]\!]$, obtained by using upwind numerical fluxes

$$\widehat{\underline{v}f} = \{\underline{v}f\} + \frac{|\underline{v}\cdot\underline{n}|}{2}[\![f]\!]$$

and analogously for $\widehat{\underline{E}f}$.

DG formulation (IV)

The same procedure can be applied to the Poisson problem (written in mixed form), yielding the following Local DG formulation

$$\int_{K_x} \underline{E} \cdot \underline{z} \, \mathrm{d}\underline{x} - \int_{K_x} \nabla\Phi \cdot \underline{z} \, \mathrm{d}\underline{x} - \int_{\partial K_x} \left(\widehat{\Phi} - \Phi\right) \underline{n} \cdot \underline{z} \, \mathrm{d}\sigma = 0$$

$$\int_{K_x} \underline{E} \cdot \nabla w \, \mathrm{d}\underline{x} - \int_{\partial K_x} \underline{n} \cdot \widehat{\underline{E}} \, w \, \mathrm{d}\sigma = - \int_{K_x} (1 - \rho) \, w \, \mathrm{d}\underline{x}$$

for $\underline{E}, \underline{z} \in \underline{Z}(K)$ and $\Phi, w \in W(K)$.

- The definition of numerical fluxes and local spaces will be considered in relation with the local energy balance.
- The form of the boundary terms is the most natural in view of deriving the local energy balance.

See [Cockburn, Shu, 1998] and [Castillo, Cockburn, Perugia, Schötzau, 2000].

SE-DG Formulation (I)

To reduce the computational cost, we can introduce a suitable quadrature rule.

- Define the 1D Gauss–Lobatto quadrature nodes and weights; the corresponding nodes and weights on K and ∂K are obtained by tensor products and affine maps.
- Using polynomials of degree k for the Vlasov equation:
  - use a quadrature formula with $k+1$ nodes
  - represent $V(K)$ using the Lagrangian basis associated with the quadrature nodes.

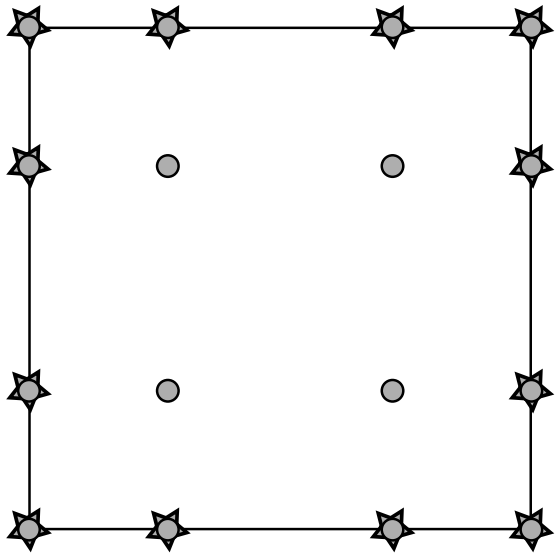

See [Kopriva, 2009] and [Restelli, Giraldo, 2009].

SE-DG formulation (II)

The SE-DG method is more efficient than the standard DG:

- the mass matrix is diagonal
- the evaluation of the numerical fluxes is simpler
- directional derivatives can be computed using “1D matrix-vector products”.

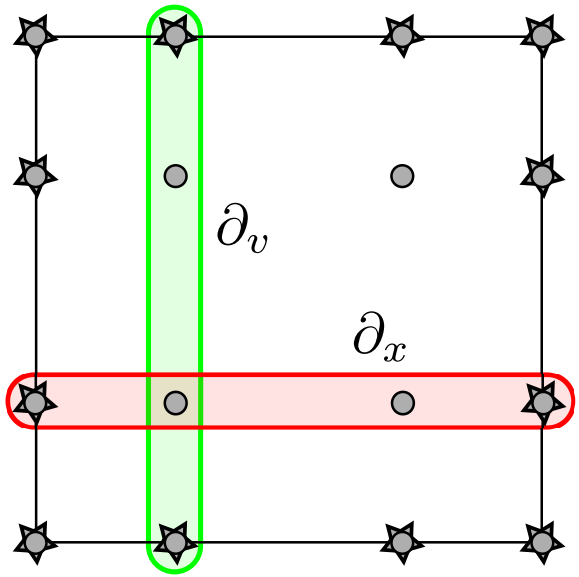

This however comes at a price: a quadrature rule with $k+1$ points is exact only for polynomials of degree $2k-1$.

Notice that all the considerations concerning particle and energy conservation are not affected by the quadrature error.

Energy balance (I)

- Let $\underline{j} = \int_{\Omega_v} \underline{v} f \, \mathrm{d}\underline{v}$, multiply the Vlasov equation by $v^2/2$ and integrate over the stripe $S_{K_x} = K_x \times \Omega_v$ to obtain the local kinetic energy balance

$$\frac{d}{dt} \iint_{S_{K_x}} f \frac{v^2}{2} \mathrm{d}\underline{x} \mathrm{d}\underline{v} = - \int_{\partial_x S_{K_x}} \underline{n} \cdot \underline{v} f \frac{v^2}{2} \mathrm{d}\sigma \mathrm{d}\underline{v} - \int_{K_x} \underline{E} \cdot \underline{j} \, \mathrm{d}\underline{x}$$

- Multiply the Vlasov equation by Φ and integrate over S_{K_x} to obtain the local electrostatic energy balance

$$\frac{d}{dt} \int_{K_x} \frac{E^2}{2} \mathrm{d}\underline{x} = \int_{K_x} \underline{j} \cdot \nabla \Phi \, \mathrm{d}\underline{x} + \int_{\partial K_x} \underline{n} \cdot \left(\underline{E}_t - \underline{j} \right) \Phi \, \mathrm{d}\sigma$$

- Adding the two equations yields the total energy balance in terms of a single valued flux on $\partial_x K$.

Energy balance (II)

We can mimic the same argument for the discrete problem. Taking as test function $u = \frac{v^2}{2}$ we obtain

$$\frac{d}{dt}\iint_{S_{K_x}} f\frac{v^2}{2}\mathrm{d}\underline{x}\mathrm{d}\underline{v} = -\int_{\partial_x S_{K_x}} \underline{n}\cdot\widehat{\underline{v}f}\frac{v^2}{2}\mathrm{d}\sigma\mathrm{d}\underline{v} - \int_{K_x}\underline{\tilde{E}}\cdot\underline{j}\,\mathrm{d}\underline{x}.$$

Taking $u = \Phi$ and using the Poisson equation we obtain

$$\begin{aligned}\frac{d}{dt}\int_{K_x}\frac{E^2}{2}\mathrm{d}\underline{x} \;&=\; \int_{K_x}\nabla\Phi\cdot\underline{j}\,\mathrm{d}\underline{x}\\ &\quad+\int_{\partial K_x}\underline{n}\cdot\left(\underline{E}_t(\hat{\Phi}-\Phi)+(\underline{\hat{E}}_t-\underline{\hat{j}})\Phi\right)\mathrm{d}\sigma.\end{aligned}$$

Notice that this requires $k \geq 2$ and $W(K) \subseteq V(K)$.

Energy balance (III)

The resulting total energy balance reads

$$\frac{d}{dt}\int_{K_x}\left[\int_{\Omega_v} f\frac{v^2}{2}\mathrm{d}\underline{v}+\frac{E^2}{2}\right]\mathrm{d}\underline{x}=\int_{K_x}\left(\nabla\Phi-\underline{\tilde{E}}\right)\cdot\underline{j}\,\mathrm{d}\underline{x}$$
$$-\int_{\partial_x S_{K_x}}\underline{n}\cdot\widehat{\underline{v}f}\frac{v^2}{2}\mathrm{d}\sigma\mathrm{d}\underline{v}$$
$$+\int_{\partial K_x}\underline{n}\cdot\left(\underline{E}_t(\hat{\Phi}-\Phi)+(\underline{\hat{E}}_t-\underline{\hat{j}})\Phi\right)\mathrm{d}\sigma.$$

Spurious energy source/sinks originate from:

- in general, $\underline{\tilde{E}}\neq\nabla\Phi$
- the energy flux on ∂K_x is not single valued.

Main idea: defining $\underline{\tilde{E}}$ to compensate these two effects.

Energy balance (IV)

It can be verified that $\underline{\tilde{E}}$ must be a function of both $\underline{x}$ *and* $\underline{v}$. In fact a balance is required between

$$\underline{\tilde{E}} \cdot \underline{j} = \underline{\tilde{E}} \cdot \int_{\Omega_v} \underline{v} f \, \mathrm{d}\underline{v}$$

and

$$\tilde{\underline{j}}\, \Phi = \Phi \int_{\Omega_v} \left(\underline{v} \{f\} + \frac{1}{2} |\underline{v} \cdot \underline{n}| [\![f]\!] \right) \mathrm{d}\underline{v}.$$

where different v-moments of f are involved.

In [Ayuso, Carrillo, Shu, 2011], different Poisson problems are solved for different values of $|\underline{v} \cdot \underline{n}|$. Here, we consider a $\underline{v}$-dependent post-processing $\underline{\tilde{E}}$ of the unique solution $\underline{E}$ of the Poisson problem.

Energy balance (V)

Cancellation of spurious energy sources is obtained by:

- use $W(K) = V(K)$ and $\underline{Z}(K) = \mathbb{RT}_k(K)$.
- use $c_{12} = 0$ and $c_{11}, c_{22} \geq 0$ in the LDG method
- define the total energy

$$\int_{\Omega_x} \left[\int_{\Omega_v} f \frac{v^2}{2} \mathrm{d}\underline{v} + \frac{E^2}{2} \right] \mathrm{d}\underline{x} + \frac{1}{2} \int_{\partial \mathcal{T}_x} \left(c_{11} [\![\Phi]\!]^2 + c_{22} [\![\underline{E}]\!]^2 \right) \mathrm{d}\sigma$$

- define

$$\underline{\tilde{E}} = \mathcal{A}\underline{E} + (\mathcal{I} - \mathcal{A}) \nabla \Phi,$$

with $\mathcal{A} = \mathrm{diag}(\alpha_1, \ldots, \alpha_d)$ and $\alpha_i(x_i) = 1 \pm \frac{2}{h}(x_i - \bar{x}_i)$, where the chosen sign depends on $|\underline{v} \cdot \underline{n}|$.

A note about DG vs. RT

The choice $W(K) = V(K)$, $\underline{Z}(K) = \mathbb{RT}_k(K)$ in the LDG method does not make it equivalent to the Raviart–Thomas method, since

- in the LDG method, $\hat{\Phi}$ is determined locally by Φ and Φ' and $\underline{E} \notin H(\mathrm{div}, \Omega_x)$
- in the Raviart–Thomas method, $\hat{\Phi}$ is an independent variable, defined by the condition that $\underline{E} \in H(\mathrm{div}, \Omega_x)$.

In both cases, however, this choice of spaces allows avoiding the stabilization, i.e. it allows the case $c_{11} = c_{22} = 0$.

See [Cockburn, Gopalakrishnan, Lazarov, 2009].

Energy balance (VI)

Notice that the choice discussed here is not unique. In fact, the relevant condition in order to eliminate the spurious energy sources is

$$\int_{K_x} \left(\nabla\Phi - \underline{\tilde{E}}\right) \cdot f\underline{v}\,\mathrm{d}\underline{x} = -\int_{\partial K_x} \left(\hat{\Phi} - \Phi\right) \underline{n} \cdot \mathcal{A} f \underline{v}\,\mathrm{d}\underline{x}.$$

This results in the total energy flux

$$\widehat{\underline{v}f}\frac{v^2}{2} + (\underline{E}_t - \underline{j}_{\mathcal{A}})(\hat{\Phi} - \Phi) + (\underline{\hat{E}}_t - \underline{\hat{j}})\Phi,$$

with $\underline{j}_{\mathcal{A}} = \int_{\Omega_v} \mathcal{A} f \underline{v}\,\mathrm{d}\underline{v}$.

It can be verified that such a flux is single valued on ∂K_x.

Time discretization (I)

After performing the space discretization, one is left with an ODE

$$\dot{\underline{q}} = \underline{F}(\underline{q}) \tag{8}$$

where $\underline{q}$ is the vector of the nodal values of f. (8) is typically discretized with an explicit RK method; we consider here the four-stage, fourth-order method

$$\begin{aligned} \underline{K}_1 &= \underline{F}(\underline{q}_n) & \underline{K}_2 &= \underline{F}(\underline{q}_n + \tfrac{\Delta t}{2}\underline{K}_1) \\ \underline{K}_3 &= \underline{F}(\underline{q}_n + \tfrac{\Delta t}{2}\underline{K}_2) & \underline{K}_4 &= \underline{F}(\underline{q}_n + \Delta t \underline{K}_3) \end{aligned}$$

$$\underline{q}_{n+1} = \underline{q}_n + \tfrac{\Delta t}{6}\left(\underline{K}_1 + 2\underline{K}_2 + 2\underline{K}_3 + \underline{K}_4\right).$$

Explicit RK methods are typically very accurate, but constrained to small Δt for stability reasons.

Exponential time integrators are a meand to reduce the computational cost, allowing larger time steps.

Time discretization (II)

For a linear ODE

$$\dot{\underline{q}} = \mathcal{A}\underline{q}, \qquad \underline{q}(0) = \underline{q}_0,$$

the solution is

$$\underline{q}(t) = e^{t\mathcal{A}}\underline{q}_0, \qquad e^{t\mathcal{A}} = \sum_{n=0} \infty \frac{1}{n!}(t\mathcal{A})^n.$$

For a nonlinear problem, the above formula can still be used as an approximation, provided $\mathcal{A}$ is substituted with the system Jacobian and the integration is performed on a small time interval.

It turns out that the matrix exponential can be computed in an efficient and accurate way by Padé polinomials, thus yielding a practical time stepping algoritm.

The resulting methods are exact for linear problems and can be made of arbitrarily high order for nonlinear ones.

See [Hochbruck, Lubich, 1997], [Sidje, 1998] and [Higham, 2005].

Time discretization (III)

For large systems, the computation of the matrix exponential would not be feasible.

Various methods have been proposed to approximate such matrix. We cosider here two options:

- projecting the exponential matrix on a relatively small Krylov space, and computing the exponential of the projected matrix $\mapsto$ computational cost proportional to the dimension of the Krylov space;
- interpolating the exponential function of a set of Leja points, and using the interpolant to evaluate the matrix exponential $\mapsto$ computational cost proportional to the number of Leja points.

Both methods can be implemented with an adaptive selction of the dimension of the Krylov space or the number of Leja points.

See [Saad, 1992], [Caliari, Vianello, Bergamaschi, 2004].

Time discretization (IV)

Both methods can be implemented in a matrix-free form.

In fact, this is obtained approximating the matrix-vector product as

$$\left(\mathcal{J}_{\underline{F}}(\underline{q})\right)\underline{v} \approx \frac{1}{\varepsilon}\left[\underline{F}(\underline{q}+\varepsilon\underline{v}) - \underline{F}(\underline{q})\right]$$

where $\mathcal{J}_{\underline{F}}$ is the Jacobian matrix, $\underline{v}$ is a generic vector and ε is a "small" parameter.

Each Krylov vector, as well as each Leja point, requires one matrix-vector product, thus implying a computational cost analogous to that of a RK stage.

see [Schulze, Schmid, Sesterhenn, 2009] and [Garcia et al., 2013].

Numerical results

We consider the follwoing test cases:

- convergence test for the Poisson solver
- linear Landau damping
- nonlinear Landau damping, 1D and 2D
- “bump-on-tail” test case
- two-stream instability.

For the precise definition of the testcases, we refer to

- *[Crouseilles, Mehrenberger, Sonnendrücker, 2010]*
- *[Guterl et al., 2010]*
- *[Ayuso, Carrillo, Shu, 2011]*.

Accuracy of $\underline{\tilde{E}}$

Accuracy of the Poisson solver, model problem

$$\partial_{xx}\Phi = -\sin(x), \quad x \in (0\,, 2\pi).$$

L^2 errors for the energy conserving reconstruction $\underline{\tilde{E}}$ for $c_{11} = \frac{c}{h}$ and $c_{11} = 0$, and for the standard LDG method, using $k = 6$.

$\log_2 n$	$\|\underline{E}_{ex} - \underline{\tilde{E}}_{h^{-1}}\|_2$		$\|\underline{E}_{ex} - \underline{\tilde{E}}_0\|_2$		$\|\underline{E}_{ex} - \underline{E}_{LDG}\|_2$	
2	$1.5 \cdot 10^{-5}$		$1.8 \cdot 10^{-5}$		$1.5 \cdot 10^{-5}$	
3	$2.4 \cdot 10^{-7}$	6.020	$2.7 \cdot 10^{-7}$	6.071	$2.3 \cdot 10^{-7}$	6.033
4	$3.7 \cdot 10^{-9}$	6.007	$4.1 \cdot 10^{-9}$	6.023	$3.6 \cdot 10^{-9}$	6.010
5	$5.7 \cdot 10^{-11}$	6.002	$6.4 \cdot 10^{-11}$	6.006	$5.6 \cdot 10^{-11}$	6.003
6	$9.0 \cdot 10^{-13}$	6.000	$9.9 \cdot 10^{-13}$	6.002	$8.7 \cdot 10^{-13}$	6.001
7	$1.4 \cdot 10^{-14}$	6.000	$1.5 \cdot 10^{-14}$	6.000	$1.4 \cdot 10^{-14}$	6.000
8	$2.2 \cdot 10^{-16}$	6.000	$2.4 \cdot 10^{-16}$	6.000	$2.1 \cdot 10^{-16}$	6.000
9	$3.4 \cdot 10^{-18}$	6.000	$3.8 \cdot 10^{-18}$	6.000	$3.3 \cdot 10^{-18}$	6.000
10	$5.3 \cdot 10^{-20}$	6.000	$5.9 \cdot 10^{-20}$	6.000	$5.2 \cdot 10^{-20}$	6.000

Landau damping

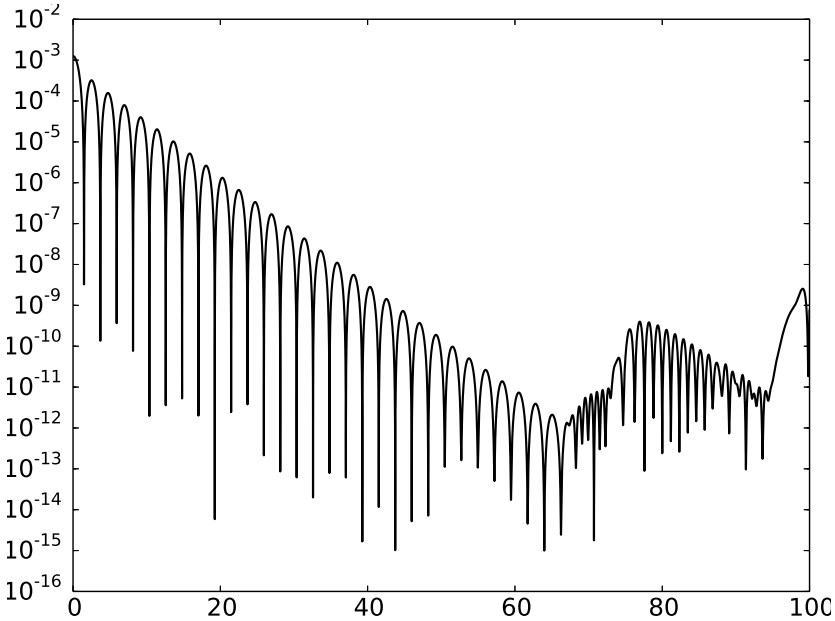

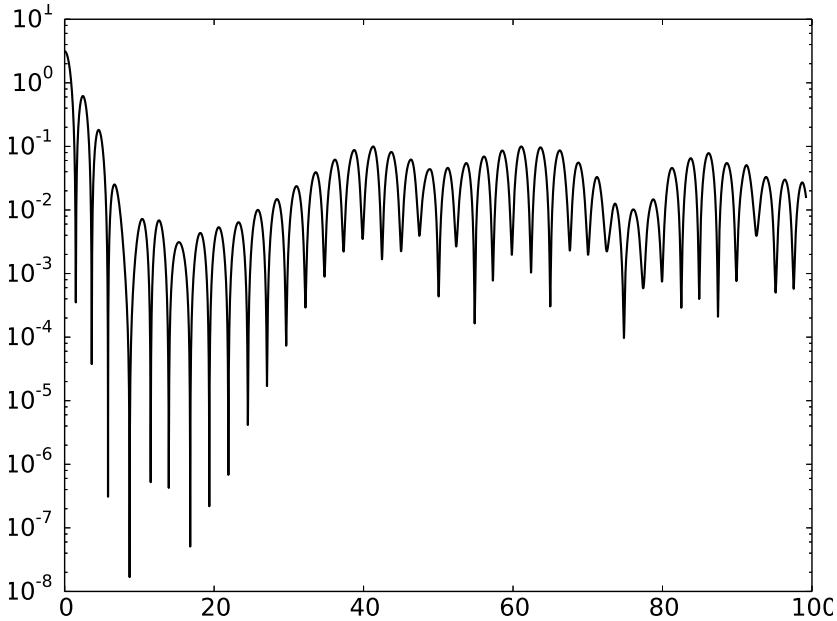

Electric energy $\frac{1}{2}\|\underline{E}\|^2$ for the linear (left) and nonlinear (right) Landau damping test cases.

$\Omega = [0\,, 4\pi] \times [-10\,, 10]$, using 50×80 elements, $k = 6$. The amplitude of the perturbation is 0.01 for the linear case and 0.5 for the nonlinear one.

Nonlinear Landau damping

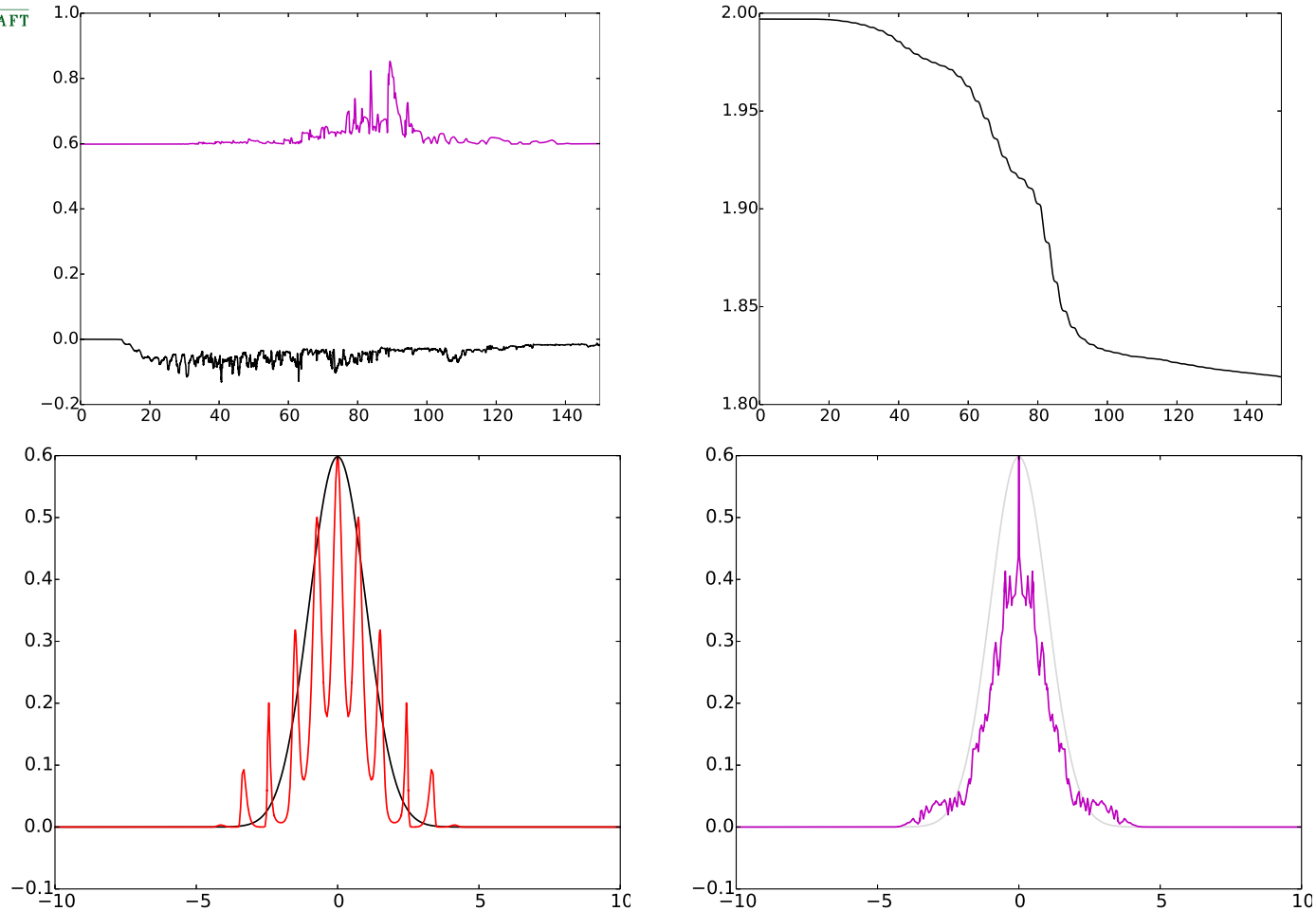

$\max_\Omega f$ and $\min_\Omega f$ (top, left), $\|f\|_2$ (top, right), section of the distribution function at $t = 0$ and 15 (bottom, left) at at $t = 150$ (bottom, right).

“Bump-on-tail” (I)

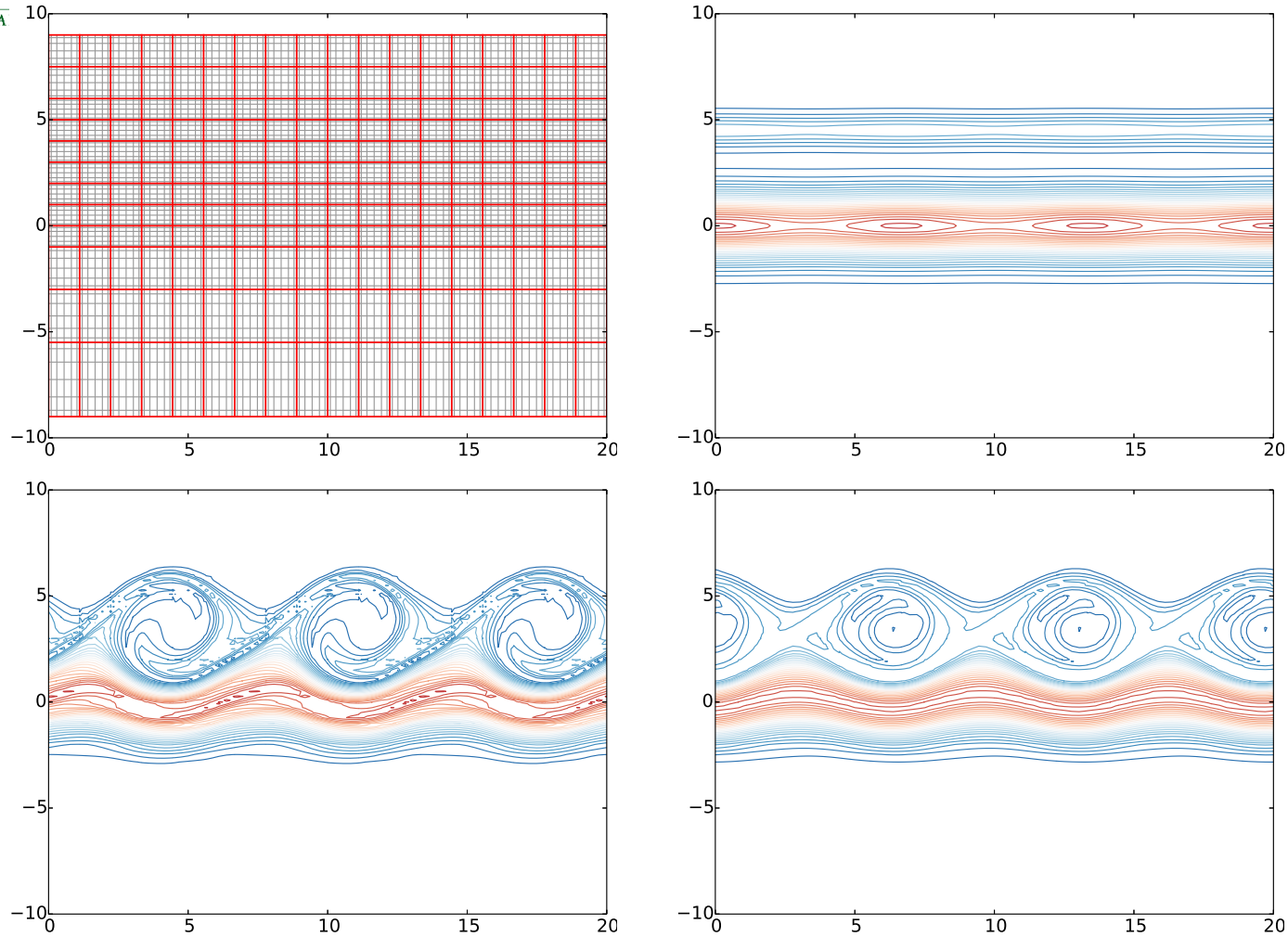

“Bump-on-tail” test case, 18×12 elements, $k = 6$. Phase space grid, initial condition and numerical solution at $t = 20$ and $t = 150$.

“Bump-on-tail” (II)

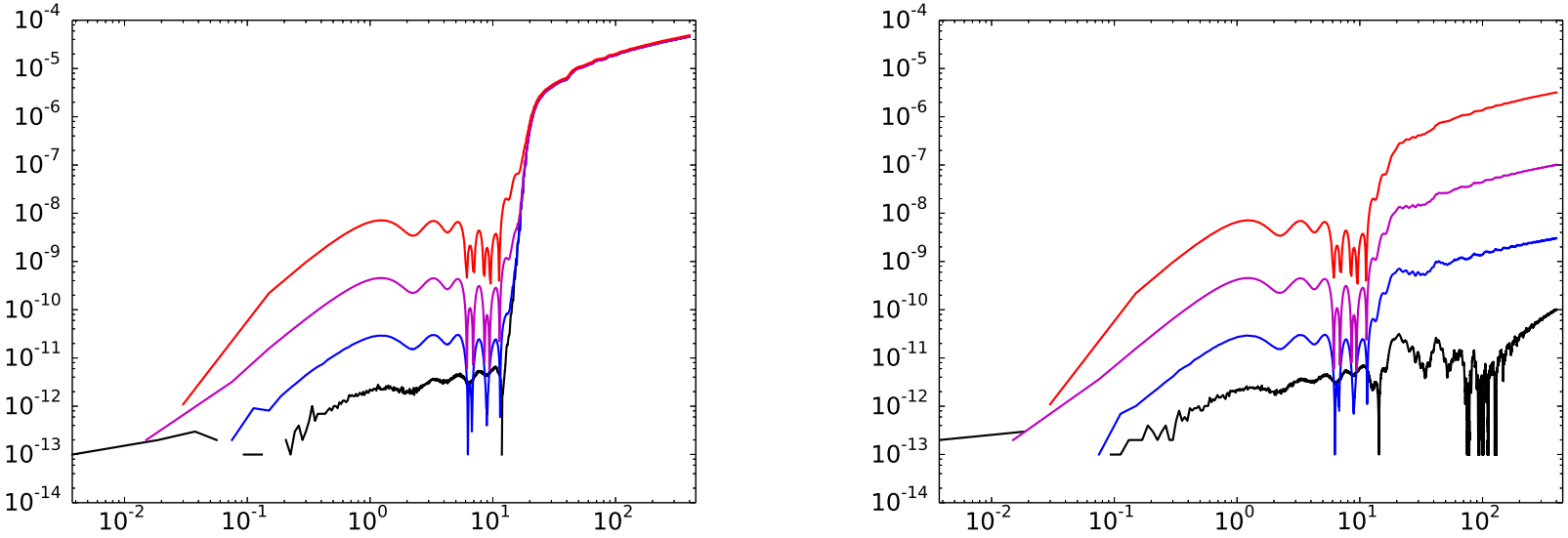

Total energy deviations for the standard upwind method (left) and the energy conserving version (right).

$\Delta t = 0.003,\ 0.007,\ 0.015,\ 0.03$ (black, blue, magenta and red).

“Bump-on-tail” (III)

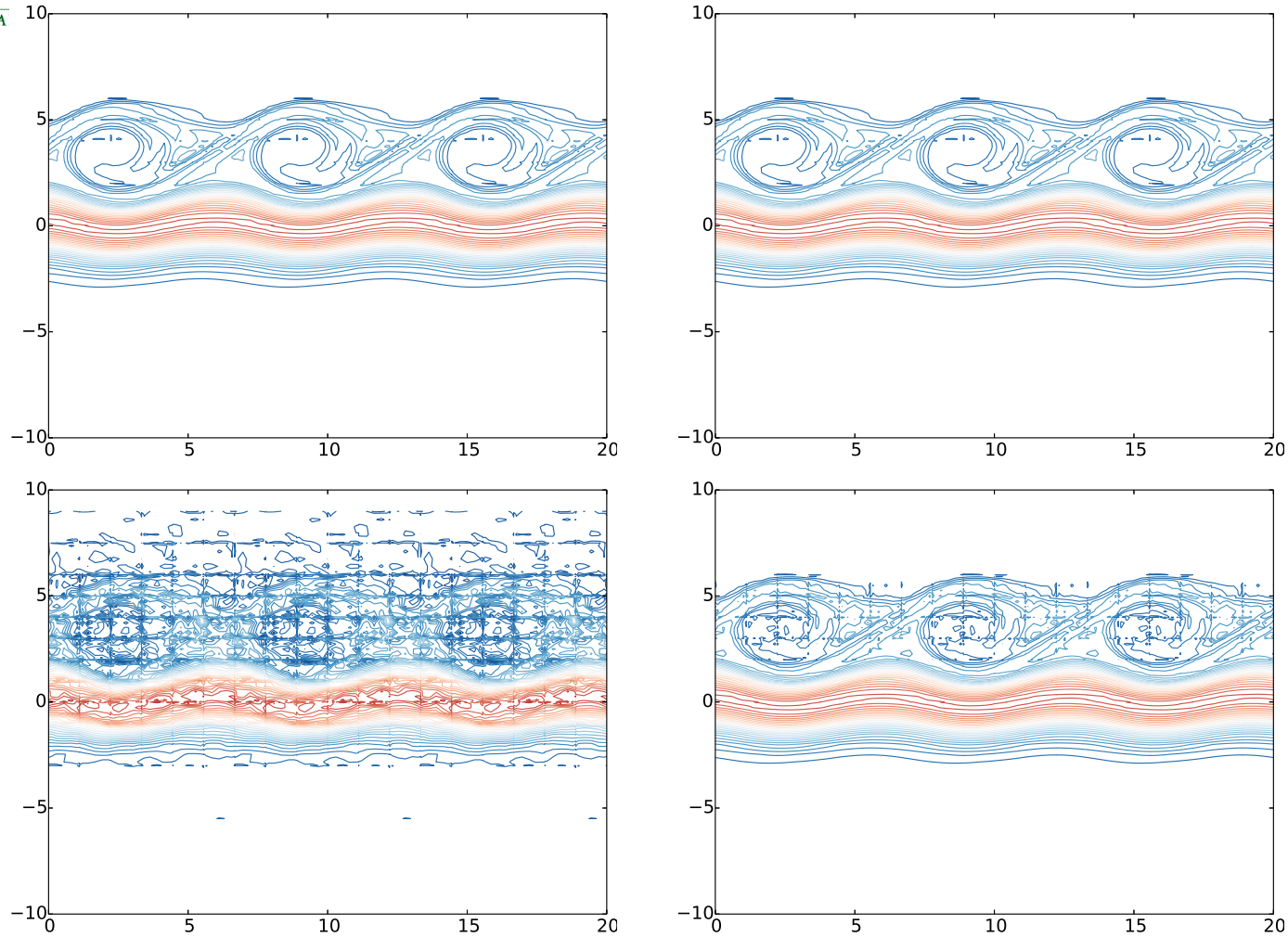

Different numerical fluxes, $t = 55$: energy conserving upwind (top left), upwind (top right), centered (bottom left) and x-centered, v-upwind (bottom right).

Two-stream instability (I)

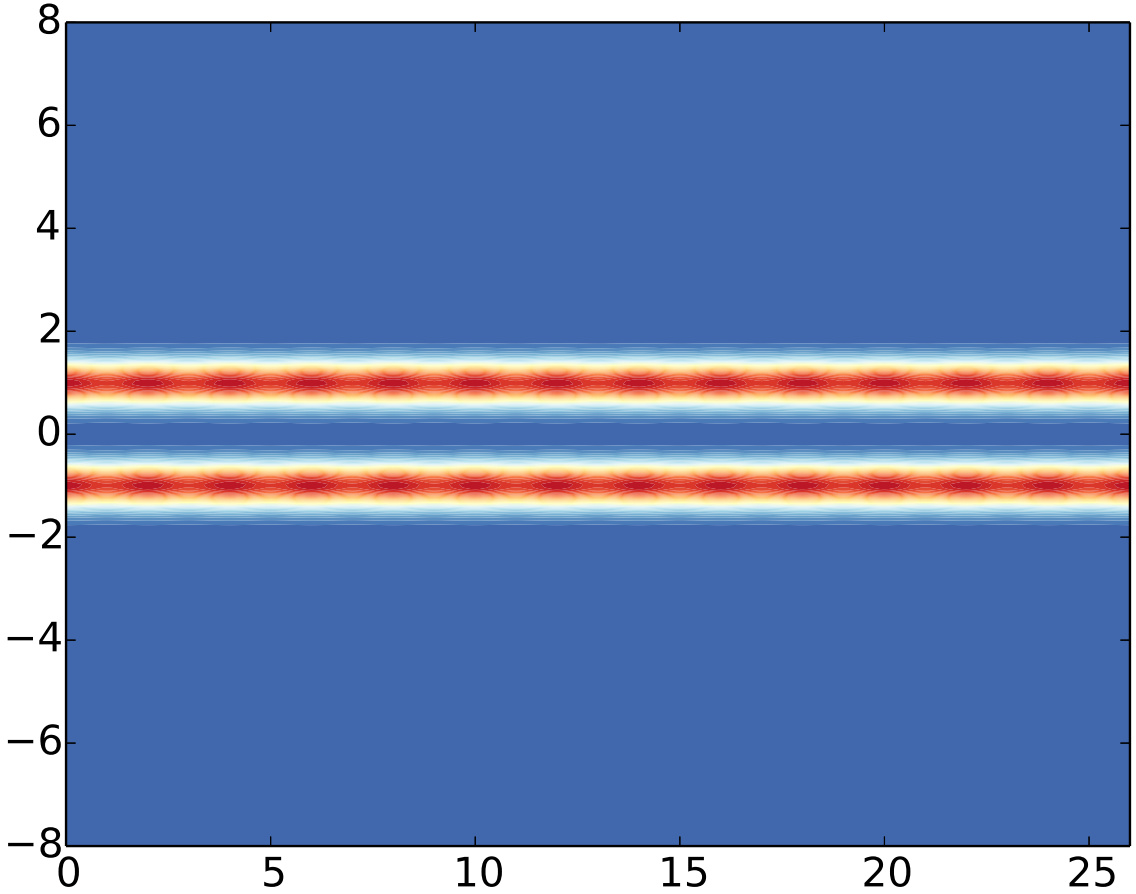

$\Omega = [0\,, 26\pi] \times [-8\,, 8]$, using 26×60 elements, $k = 5$. Initial condition.

Two-stream instability (I)

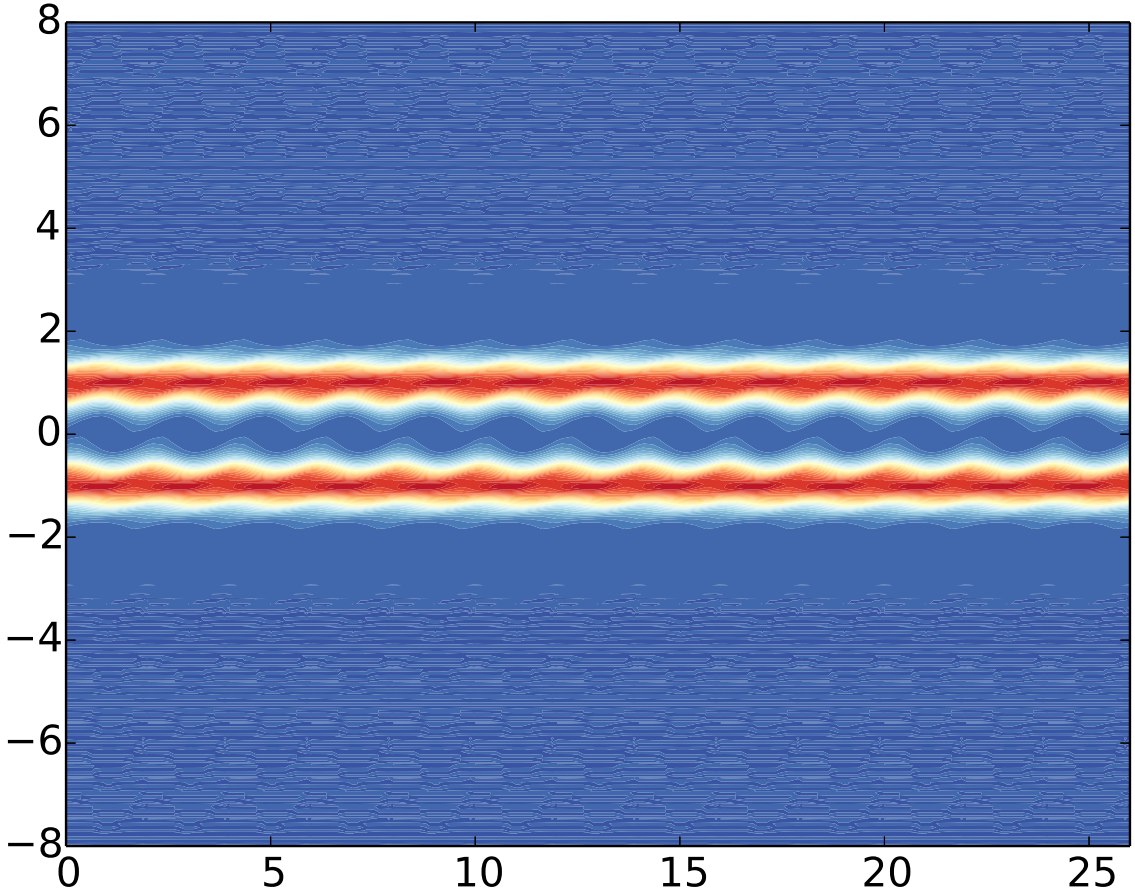

$t = 10$

Two-stream instability (I)

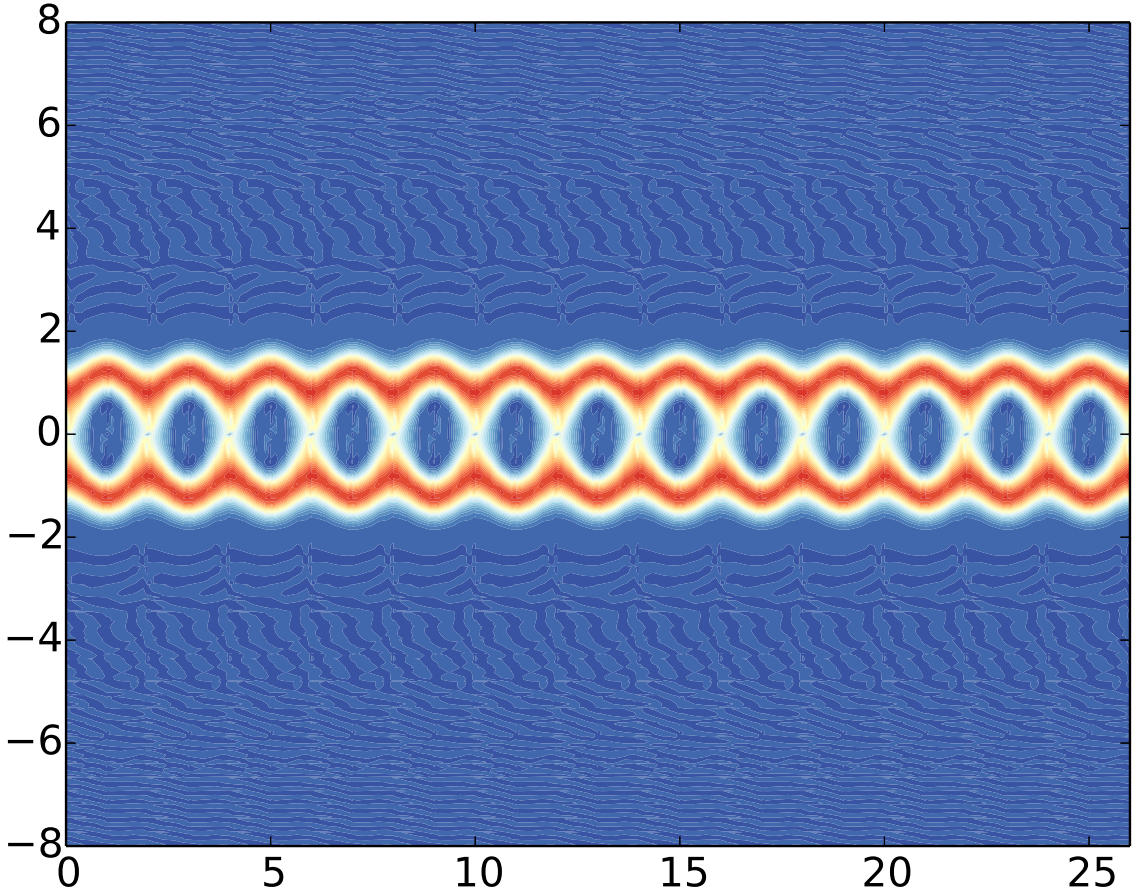

$t = 30$

Two-stream instability (I)

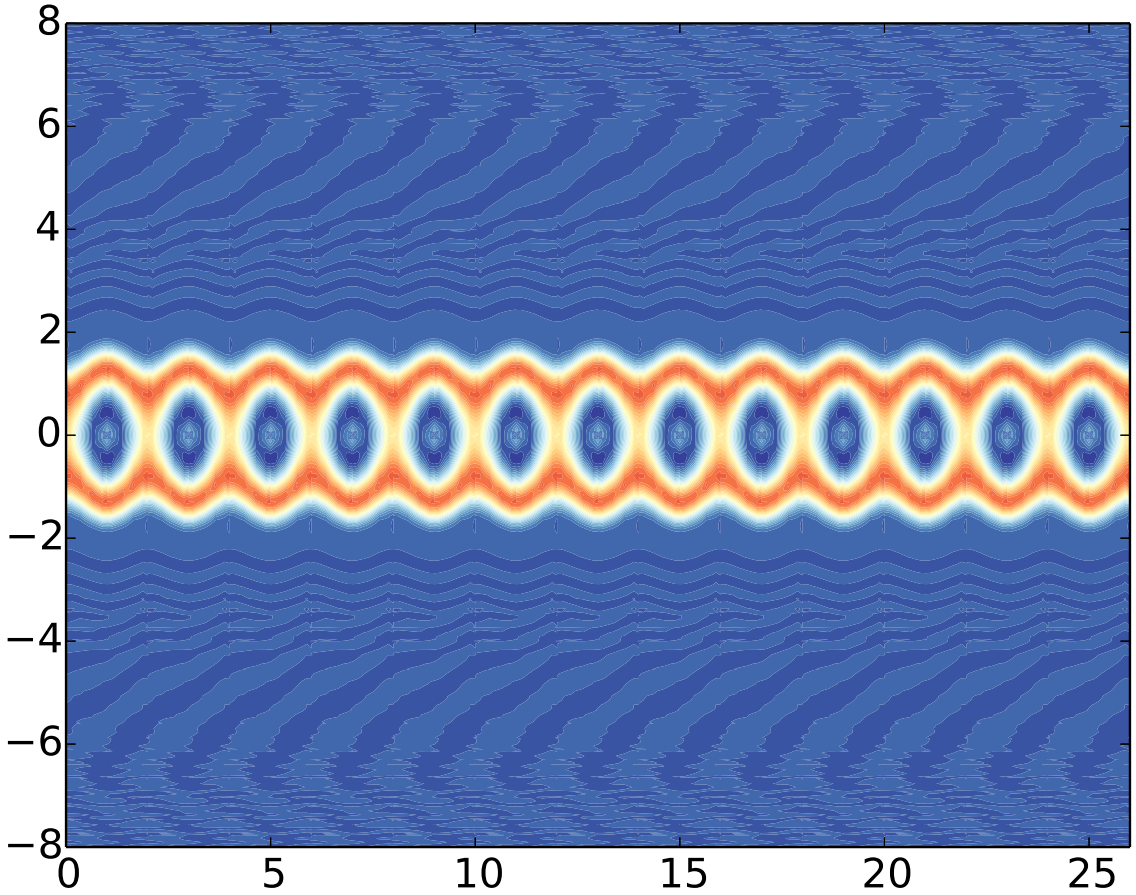

$t = 70$

Two-stream instability (I)

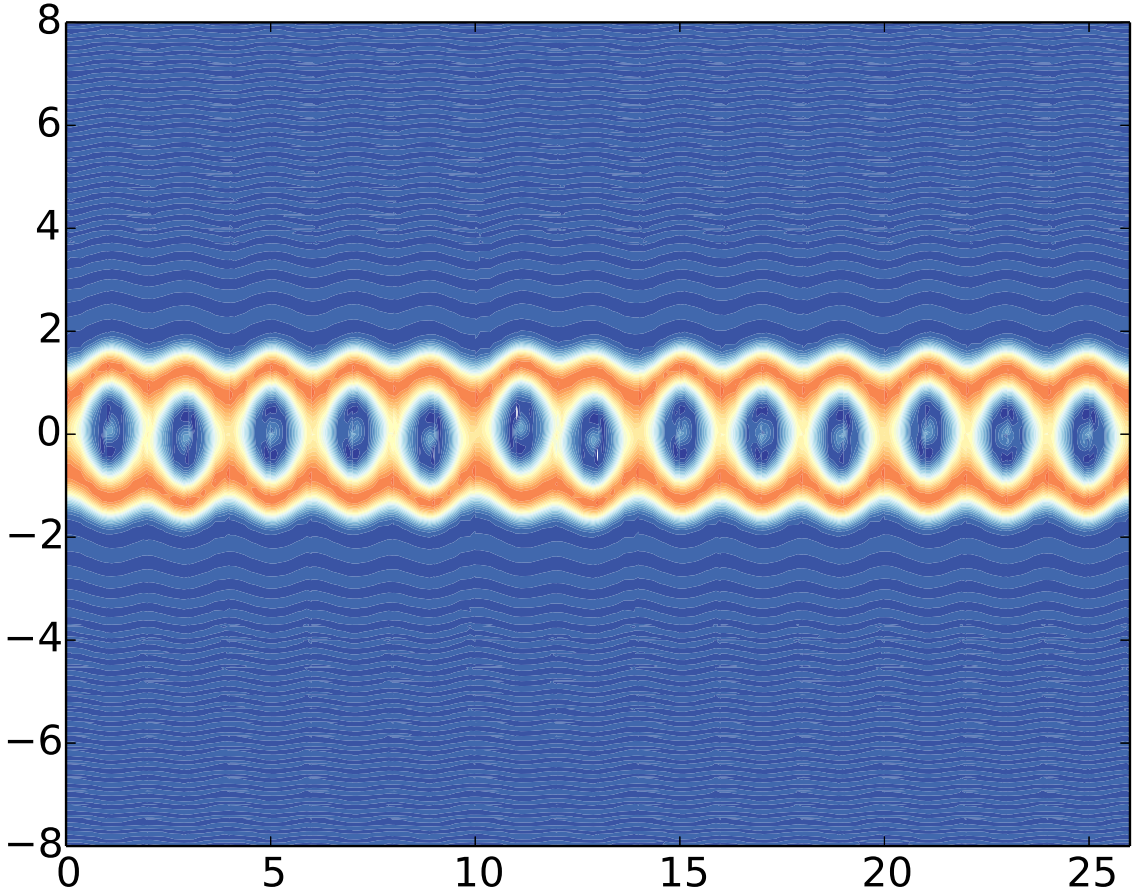

$t = 130$

Two-stream instability (I)

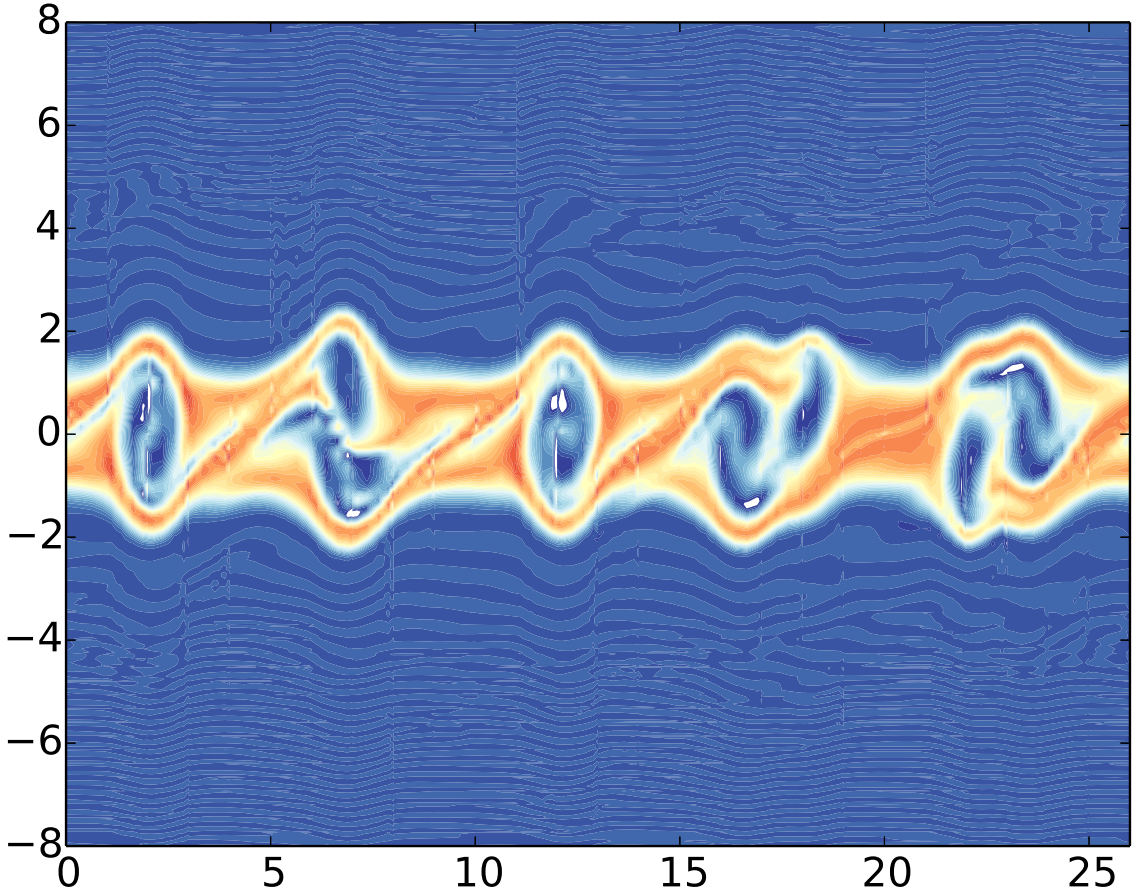

$t = 150$

Two-stream instability (I)

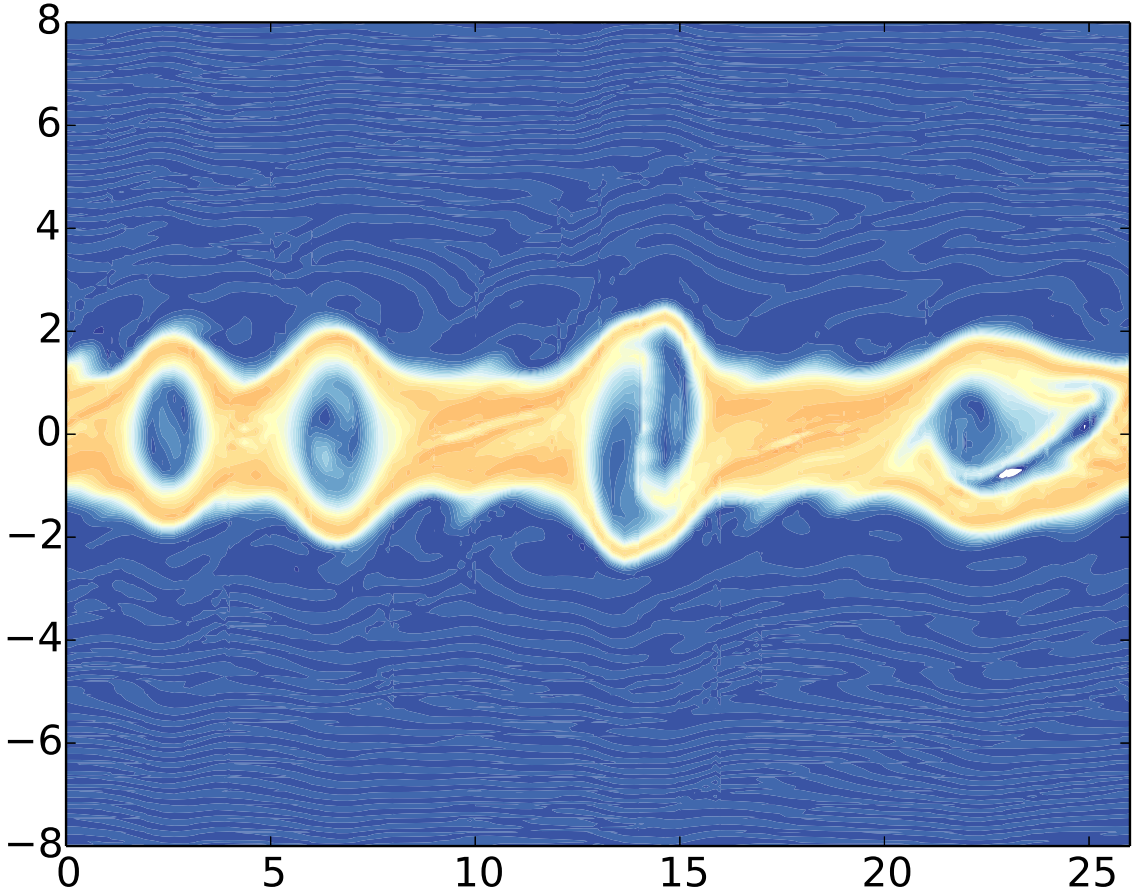

$t = 200$

Two-stream instability (I)

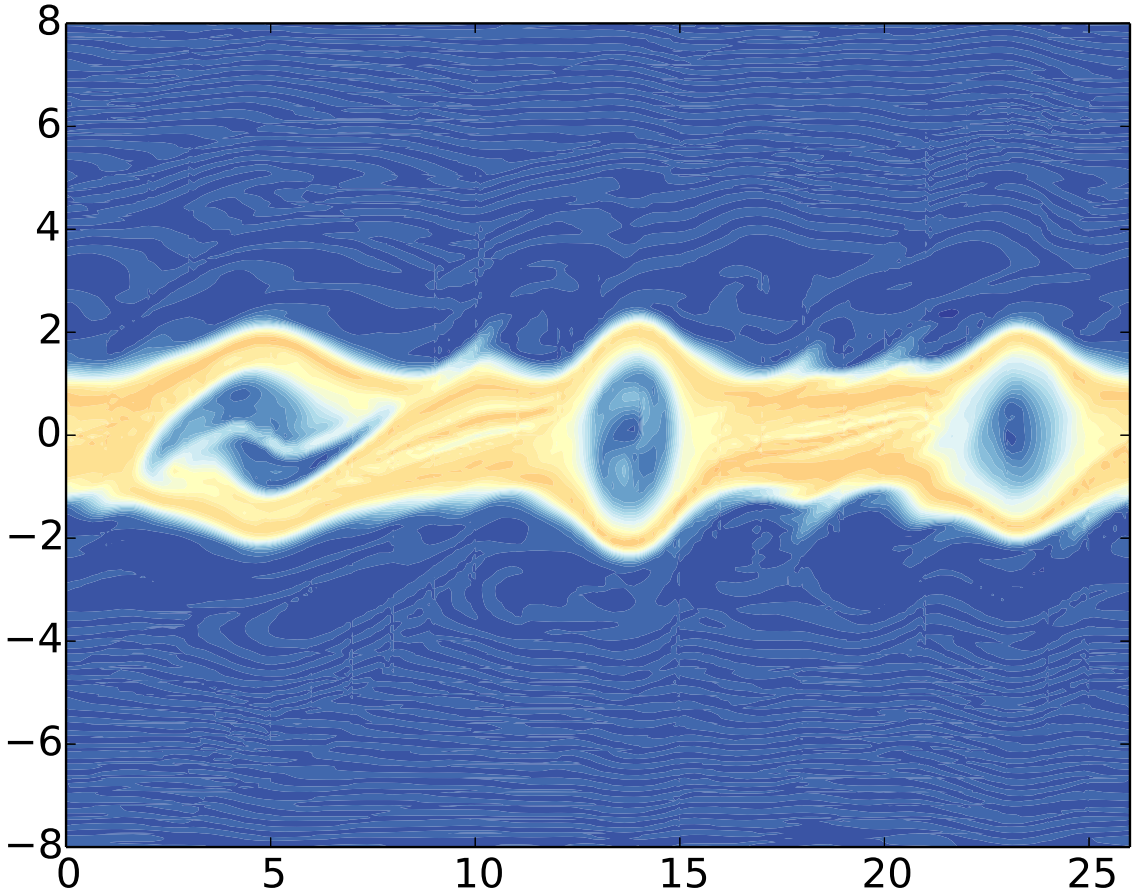

$t = 250$

Two-stream instability (I)

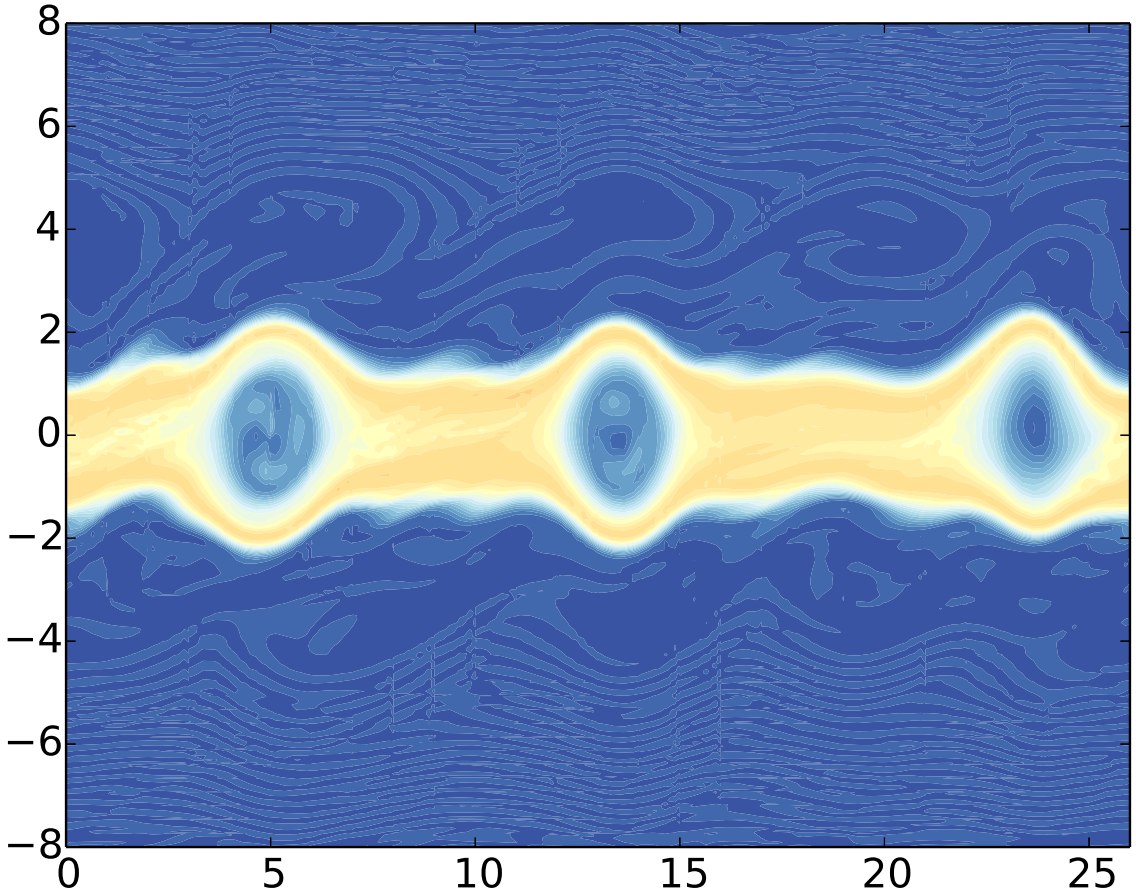

$t = 300$

Two-stream instability (I)

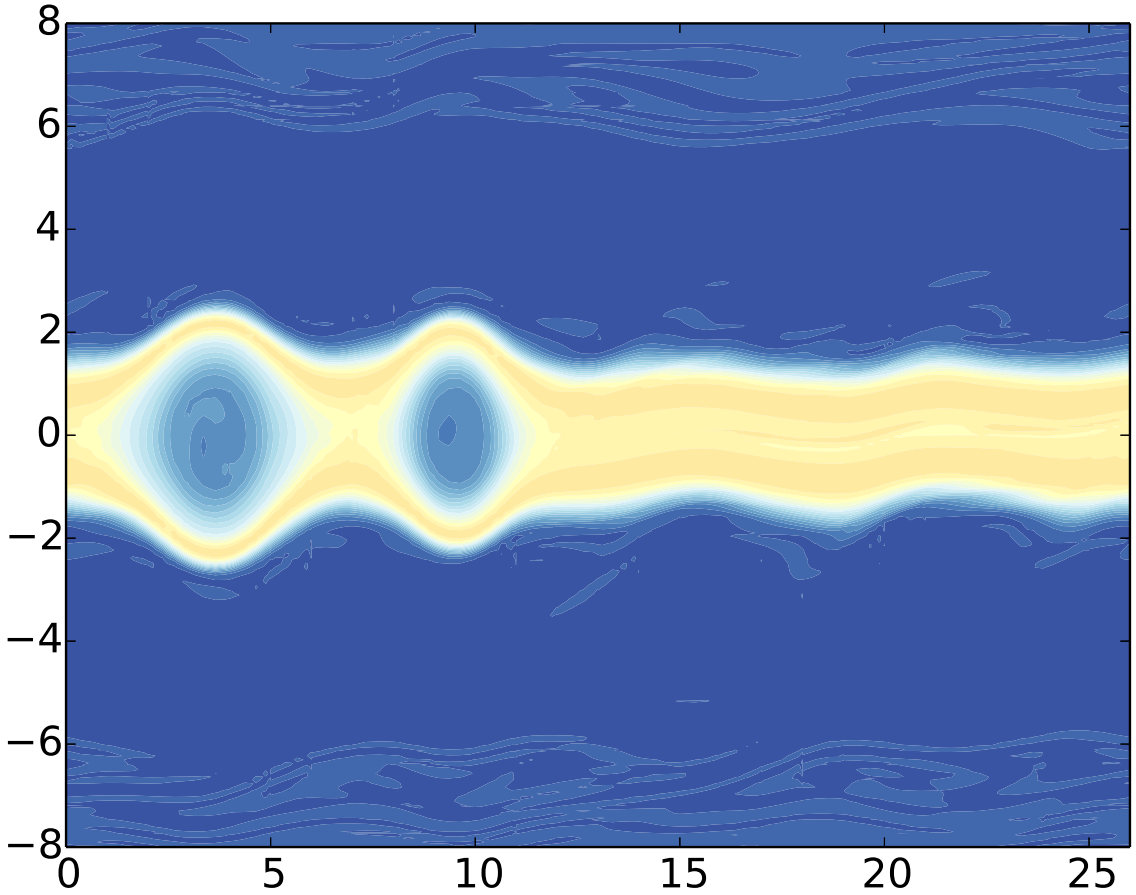

$t = 750$

Two-stream instability (I)

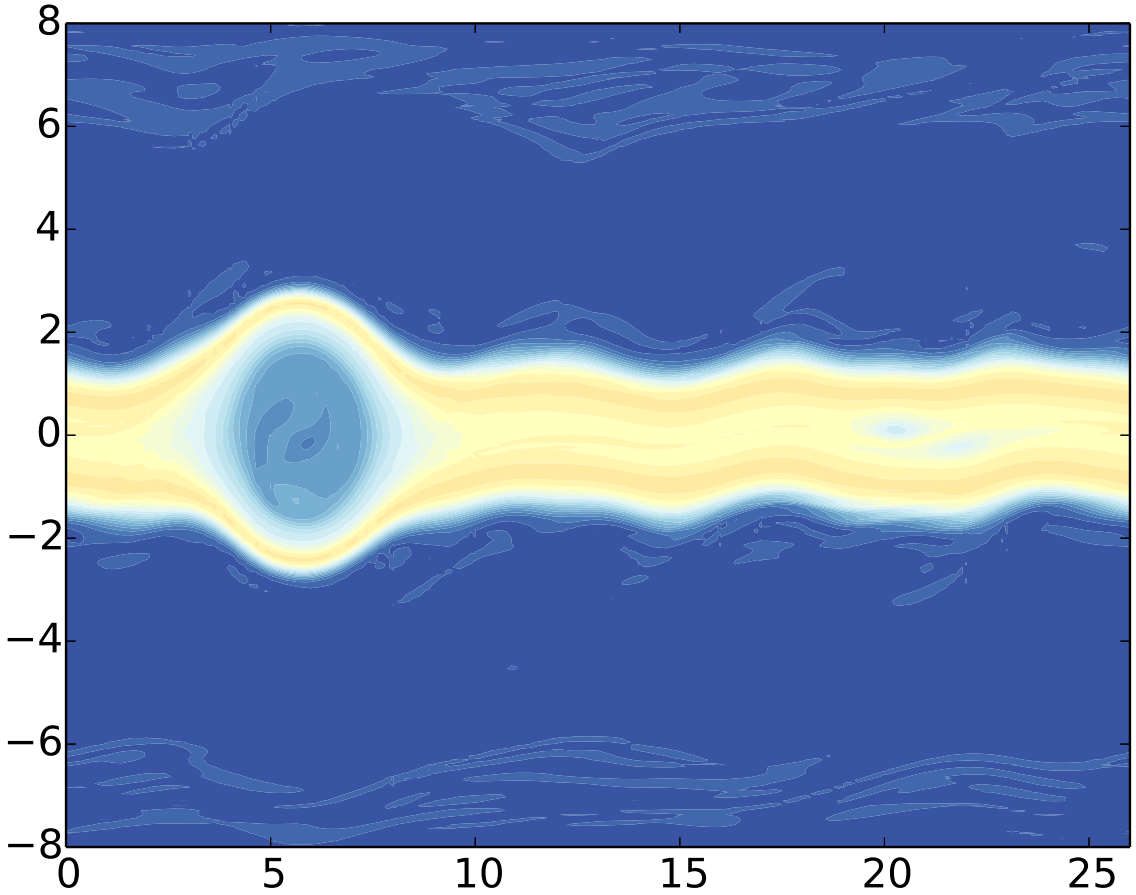

$t = 1000$

Two-stream instability (II)

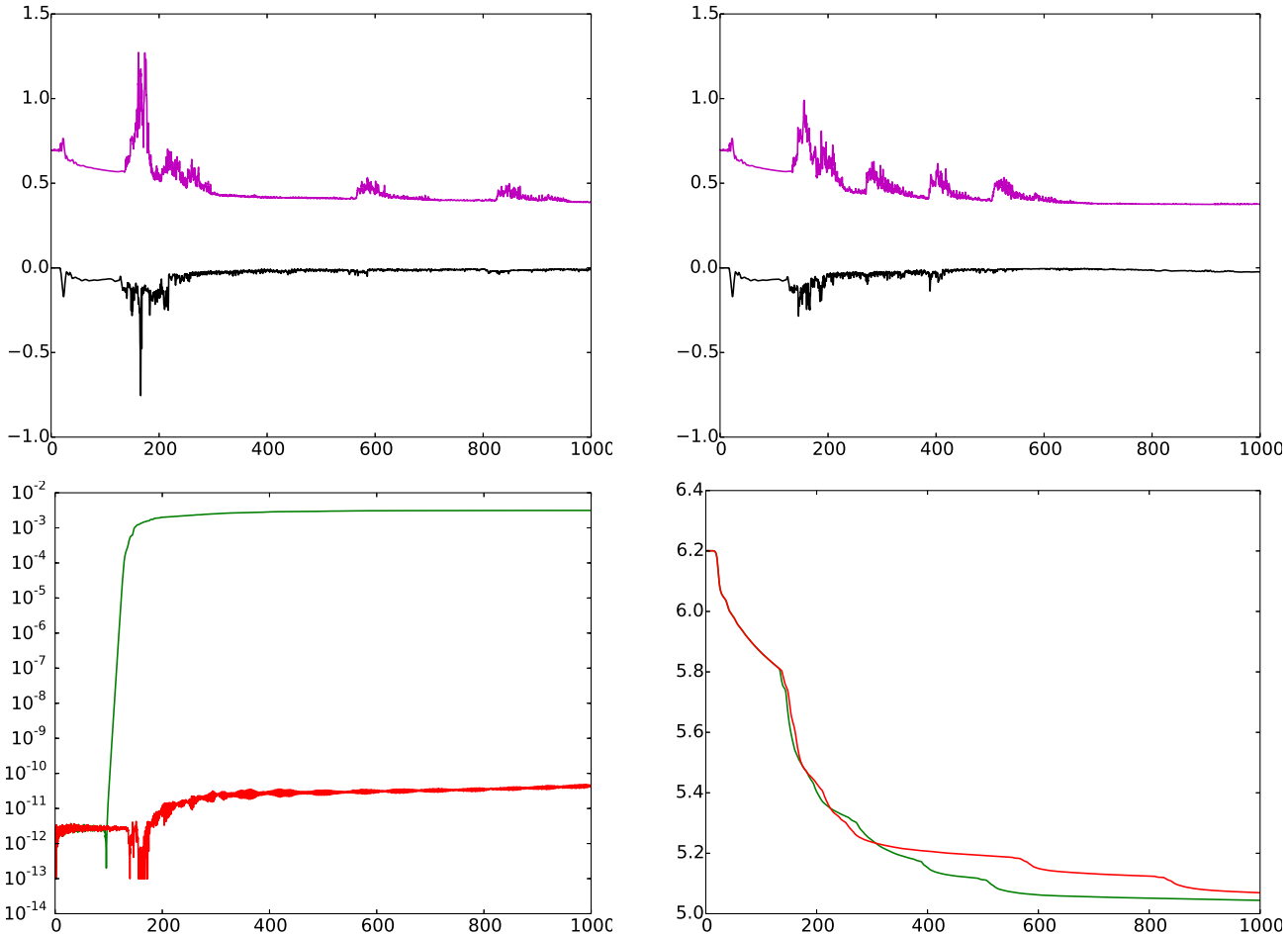

First row: $\max_\Omega f$ and $\min_\Omega f$ for the energy conserving (left) and the standard upwind (right) schemes.

Second row: total energy deviation (left) and $\|f\|_{L^2}$ (right) for the energy conserving (red) and the standard (green) upwind schemes.

2D Landau damping (I)

We consider a 2D version of the nonlinear Landau damping.

- $\Omega_x = [0\,, 4\pi]^2$, $\mathcal{T}_x$: 8×4, $k = 5$;
- $\Omega_v = [-9\,, 9]^2$, $\mathcal{T}_v$: 12×8, $k = 7$, refined;
- total number of elements: 3072, total number of points: 7077888.

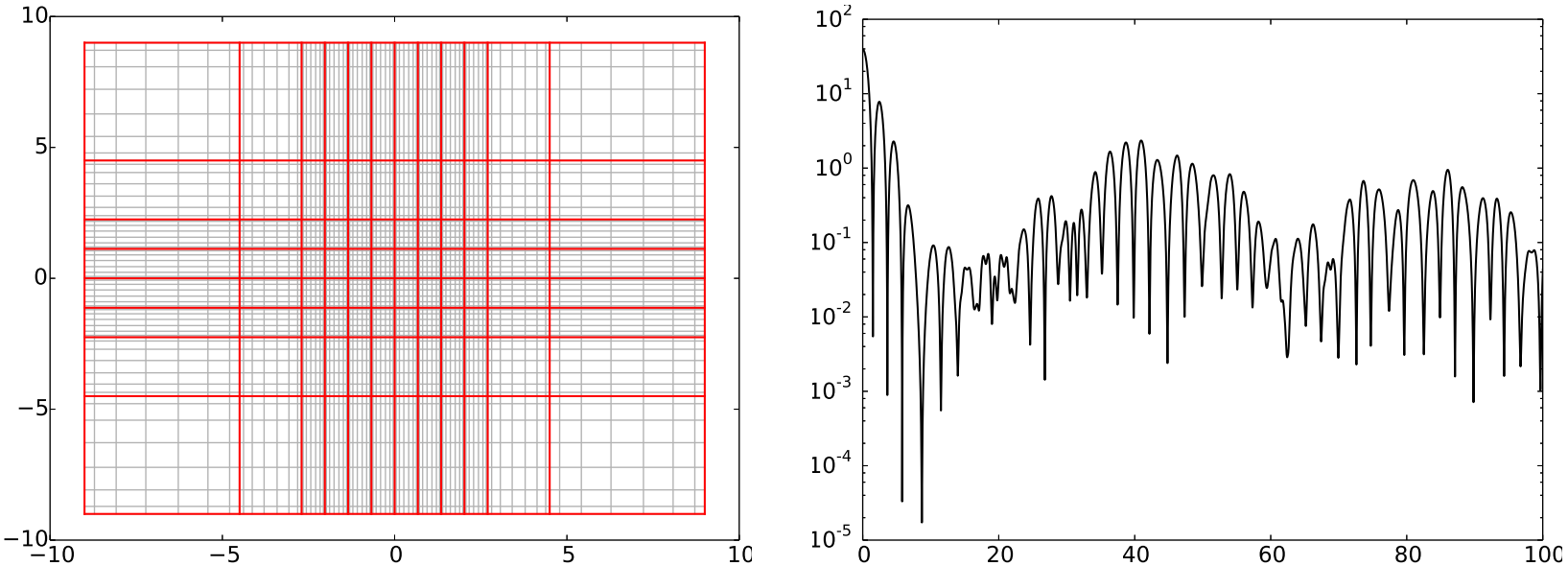

Velocity space grid (left) and electric energy evolution (right).

2D Landau damping (II)

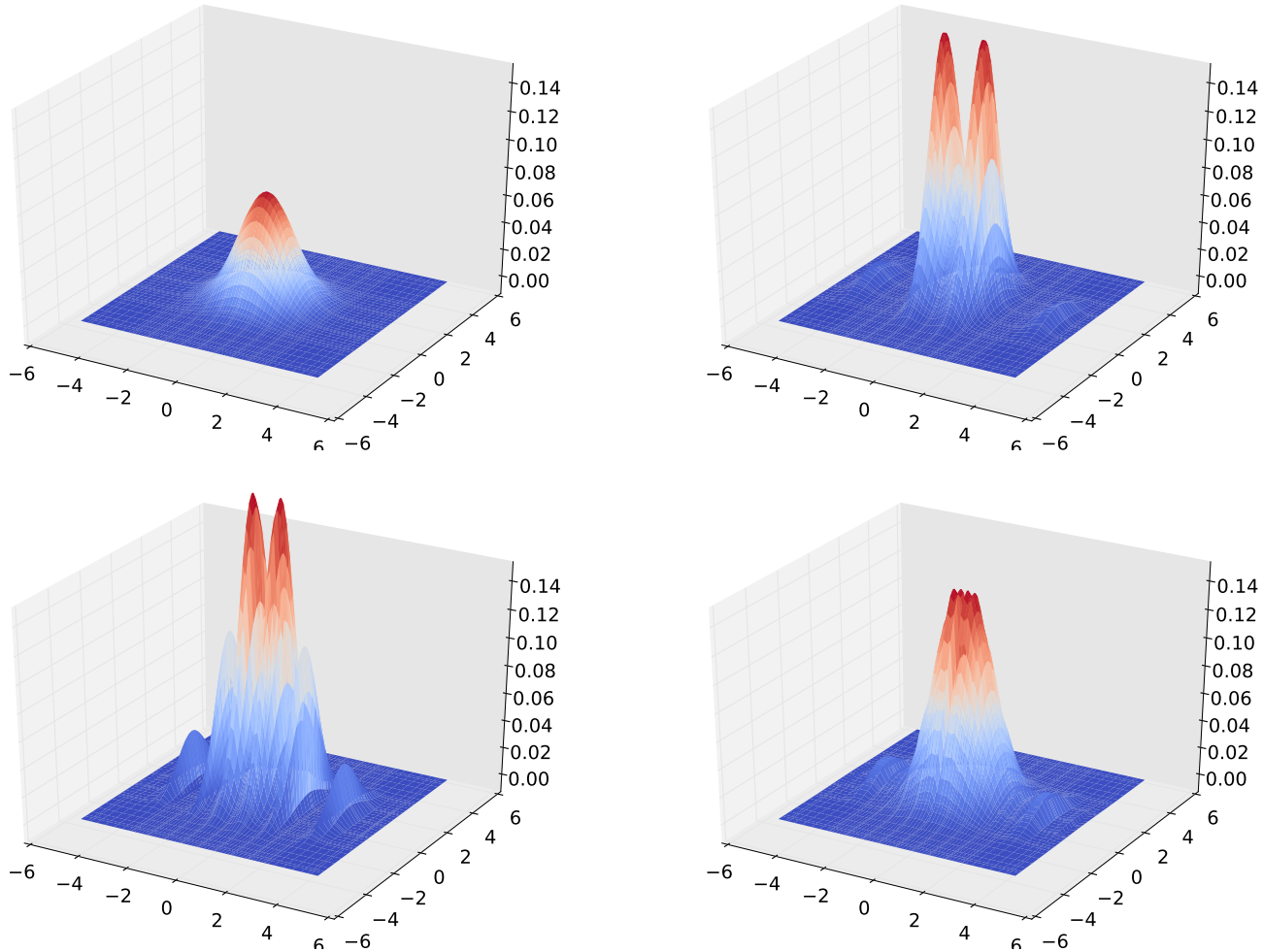

Distribution section at fixed $\underline{x}$ at time levels 0, 5, 10 and 150.

Exponential intergrator (I)

For the two-stream instability test, RK time discretization requires $\Delta t^{RK} = 0.1$ with error $\|f_{ex} - f\|_2 = 7.1 \cdot 10^{-5}$, where f_{ex} is the solution of the discrete in space, continuous in time system.

For the same problem, defining the effectivity index

$$\eta = \frac{5}{\Delta t^{RK}} \frac{\Delta t^{exp}}{n^{exp}}, \qquad n^{exp} = \text{rhs evaluations},$$

	$\epsilon = 10^{-3}$		$\epsilon = 10^{-6}$		$\epsilon = 10^{-9}$	
Δt^{exp}	$\|f_{ex} - f\|_2$	η	$\|f_{ex} - f\|_2$	η	$\|f_{ex} - f\|_2$	η
0.05	$4.26 \cdot 10^{-3}$	0.83	$7.02 \cdot 10^{-5}$	0.50	$3.76 \cdot 10^{-5}$	0.37
0.1	$8.48 \cdot 10^{-3}$	1.44	$1.49 \cdot 10^{-4}$	0.86	$1.49 \cdot 10^{-4}$	0.61
0.2	$1.11 \cdot 10^{-3}$	1.98	$5.81 \cdot 10^{-4}$	1.35	$5.81 \cdot 10^{-4}$	0.95
0.4	$2.31 \cdot 10^{-3}$	2.31	$2.21 \cdot 10^{-3}$	1.72	$2.21 \cdot 10^{-3}$	1.37
1.0	$1.18 \cdot 10^{-2}$	2.62	$1.18 \cdot 10^{-2}$	2.16	$1.18 \cdot 10^{-2}$	1.84

Exponential integrator (II)

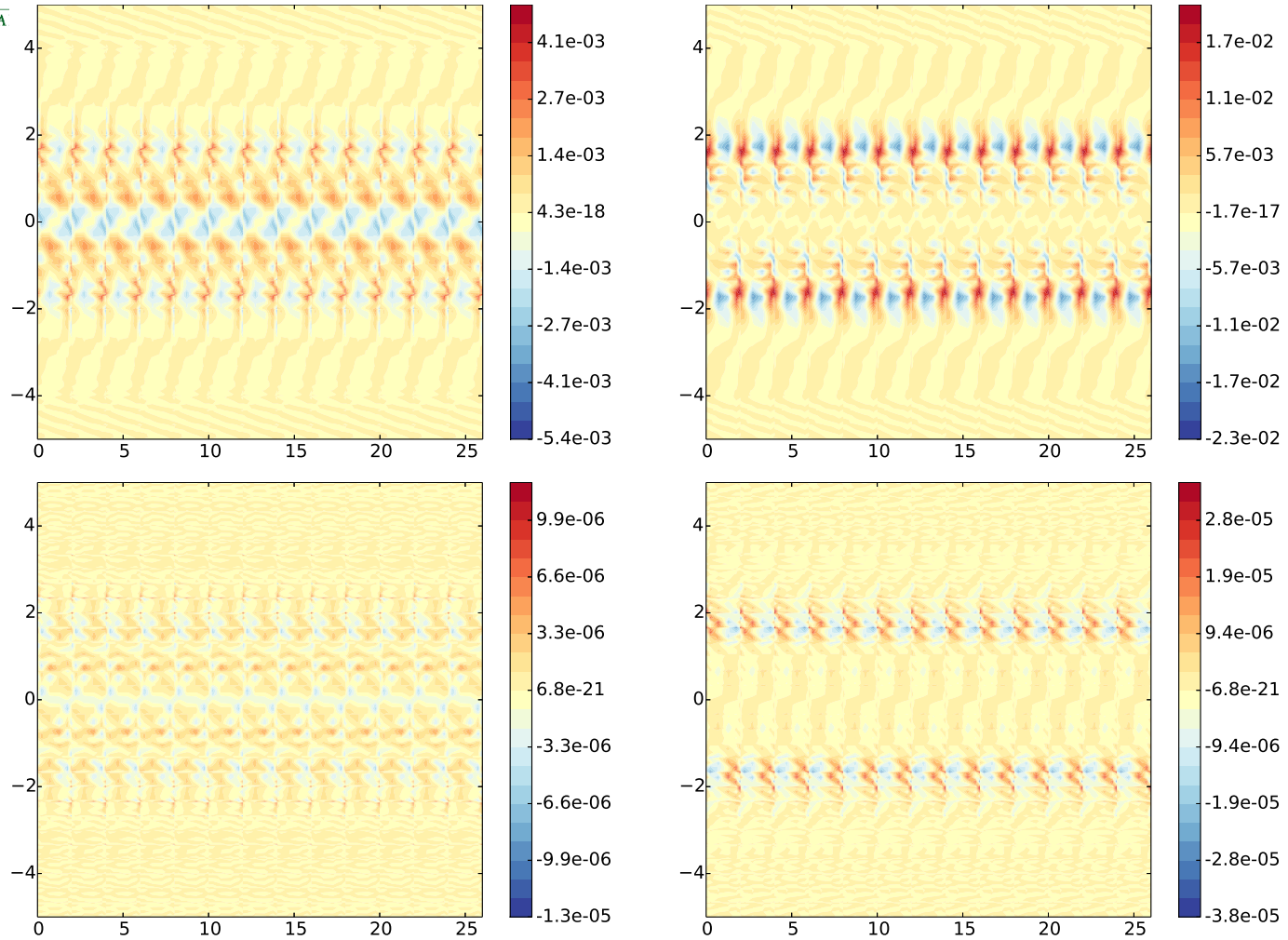

Two-stream instability: converge of the Krylov space (left) and Leja point (right) methods. Error plots for f after 5 iterations (top) and 18 iterations (bottom).

Conclusions

We have discussed a SE-DG method for the Vlasov–Poisson equation. The method provides

- particle conservation (by construction)
- energy conservation (thanks to the use of a reconstructed electric field in the Vlasov equation)

For the time discretization, two alternatives have been considered: Runge–Kutta methods (the standard solution) and exponential integrators based either on Krylov space projection or on Leja point interpolation.

Future development will concern:

- extension to nonconforming grids
- introduction of limiters, possibly along the lines of [Zhang, Shu, 2010].